

Emulation of Conducted Emissions of an Automotive Inverter for Filter Development in HV Networks

M. Reuter^{1*}, T. Friedl, S. Tenbohlen¹, W. Köhler¹

¹ Institute of Power Transmission and High Voltage Technology (IEH), University of Stuttgart, Germany

*Martin.Reuter@ieh.uni-stuttgart.de

Abstract — At present, electric traction systems are introduced into automotive applications. The driving power is transmitted via cables, which are routed close to various communication, sensor or control units. Ensuring the electromagnetic compatibility (EMC) of these miscellaneous systems within the electric vehicle is a new challenge for the developing engineers. Line filters are a very effective EMC measure, but a time-consuming and ineffective trial-and-error approach can only be avoided if the input and output impedances of the filters are characterized and known.

This paper characterizes the impedance situation for a line filter within a high voltage traction system. It is intended to reduce the conducted emissions of a power inverter for a hybrid driven car. Therefore, the inverter's common and differential mode input impedances are determined. The tested device is modeled as a voltage source combined with an inverter emulating network of concentrated elements. Verifying measurements show that the inverter's EMC performance can be reproduced with the presented inverter emulation. The influence of the changed impedance situation on the attenuation of a first-order low-pass filter is shown by emission measurements.

Keywords - Electric Vehicles, EMC of HV Systems, Traction Inverter Model, Disturbance Source Emulation, Filter Attenuation

I. INTRODUCTION

The increasing electrification of the traction system for electric driven vehicles leads to new issues in controlling the entire system's EMC [1]. Most recent concepts of hybrid driven cars combine an electric machine with a combustion engine in the front motor compartment. The required traction battery is usually placed underneath the rear trunk. Therefore, a transmission of electric power through the entire car is needed by a cable harness of about 3 – 4 m length. To reduce ohmic losses of the transmission, the operating voltages are increased up to 120 – 400 V_{DC}. These boundary conditions lead to unintended electromagnetic interferences (EMI) between the traction system and surrounding susceptible radio frequency (RF) communication systems, such as the reception of FM radio. The high voltage (HV) traction network is assembled entirely shielded to control the EMC of the miscellaneous systems situated close to each other. Further reduction of unintended interference can be achieved by lowering the conducted emissions of the traction system with line filters.

An effective filter design requires the knowledge of load and source impedances [2]. Norton's and Thévenin's theorems state the equivalence of any electrical network to one ideal voltage source combined with a series impedance, respectively a current source with a parallel resistor [3]. Thus any linear

source of conducted emissions can be modeled by a voltage source and a series impedance. This leads to the perception that the amplitudes of conducted emissions are determined mainly by three factors: the amplitude of the equivalent voltage source, its source impedance and the value of the load impedance [4]. The load situation within EMC tests for HV components is known [5]. A reduction of EMI using line filters requires a characterization of the disturbance sources inside the power inverter, as it is the main source of electromagnetic emissions within the electric traction system.

This contribution determines the input impedance of a traction inverter for a hybrid driven car in its passive state, i.e. switched off and unconnected as a black box model. Time domain measurements allow the calculation of source voltage and series impedance of the active device at a typical operating point. The common mode (CM) impedance measured in the passive state is then verified to be equivalent to the disturbance source's series impedance of the active inverter. Knowledge of CM and differential mode (DM) impedances allows the development of an EMC simulation model. The influence of the inverter's input impedances on the attenuation of a first-order low-pass EMI filter is shown.

II. IMPEDANCE CHARACTERIZATION OF AN AUTOMOTIVE INVERTER AS A PASSIVE TWO-PORT

The input impedances of the investigated inverter are calculated based on network analyzer (VNA) measurements.

A. Impedance Calculation using Scattering Parameters

The device under test (DUT) is composed of a pulse width modulated B6-bridge and a DC/DC-converter for a low voltage (LV) on-board power supply. The differentiation between CM and DM input impedances is made for EMC issues. Figure 1 shows a simplification of the inverter's electric network to an EMC equivalent circuit of CM and DM impedances.

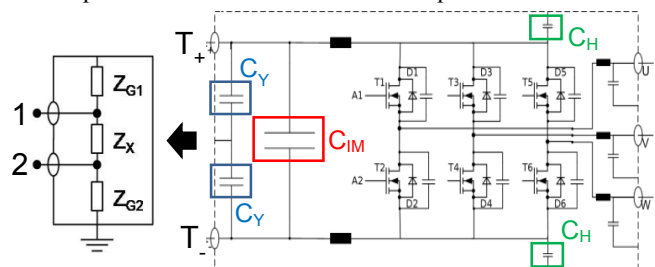


Figure 1. Simplified equivalent circuit of the inverter, consisting of common mode impedances Z_{G1} , respectively Z_{G2} , and differential mode impedance Z_X

In the equivalent circuit shown in Figure 1, Z_{G1} and Z_{G2} correspond to the CM impedances. Z_X represents the DM impedance. The internal structure of the inverter consists of two input capacitors (C_Y), an intermediate circuit capacitor (C_{IM}), parasitic capacitances to the housing (C_H), and six semiconductor IGBTs, forming a B6-bridge ($T_1 - T_6$). The black box behavior of the inverter's inner construction is equivalent to the three presented complex impedances.

A VNA is used to measure the scattering parameters of the inverter at the traction supply ports 1 and 2 (T_+ / T_-) of Figure 1. A mathematical conversion of the scattering parameters is necessary for a calculation of the three impedance values Z_X , Z_{G1} and Z_{G2} . Firstly, the impedance parameter matrix $[Z]$ is calculated as described in [6]. The designated CM and DM impedances are determined with these Z-parameters using the equation system shown in Figure 2.

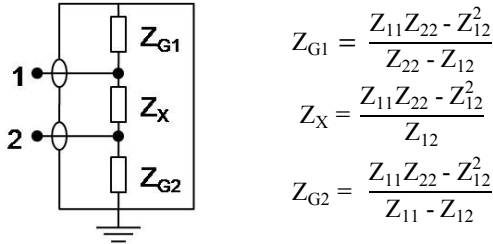


Figure 2. Equivalent circuit and calculation methodology of common mode and differential mode impedances using Z-parameters

As the direct scattering parameter measurements can only be executed for passive devices, the DUT is investigated in an unpowered state with no HV or LV harnesses attached. The resulting impedance curves of Z_X , Z_{G1} and Z_{G2} are plotted in Figure 3.

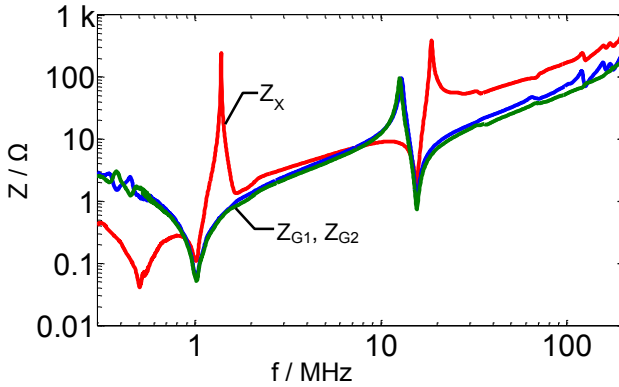


Figure 3. Impedance curve of the HV inverter analyzed in the passive state using an Agilent ENA E5070B network analyzer

It can be seen that Z_{G1} and Z_{G2} have a similar characteristic over the whole frequency range, suggesting a symmetric structure inside the power inverter. Therefore, in the following, only the impedance Z_{G1} is examined and all statements obtained also apply to Z_{G2} . The CM impedances begin at several ohms and have a minimum value of 50 mΩ at 1 MHz. An inductive impedance increase occurs above this main series resonance, peaking at ~12 MHz. A second series resonance follows at 15 MHz, continued by a further inductive impedance increase. Thus, a connection in parallel of two series resonance

circuits is assumed. The first series resonance at 1 MHz is traced to the capacitor C_Y interacting with the parasitic inductance of the capacitor and its wiring. The second series resonance at 15 MHz is formed by the total housing capacitance C_H and the inductance of the connection between power semiconductors and C_Y . The cross coupling impedance Z_X also starts with a capacitive behavior, having a first resonance at about 500 kHz. This series resonance is followed by an impedance peak at 800 kHz. The series resonance of C_Y also occurs in Z_X , as the series connection of both C_Y forms a low resistive path between the two ports T_+ and T_- . This minimum impedance at 1 MHz is followed by a parallel resonance at about 1.5 MHz with a significantly high Q-factor. An inductive impedance increase occurs above this frequency with a series resonance at 15 MHz and a parallel resonance at 20 MHz. Above 20 MHz, an inductive impedance trend can be observed with multiple, but insignificant resonances.

B. Development of a SPICE Simulation Model

The EMC equivalent impedances determined for CM and DM allow a “grey box” modeling approach of the inverter’s RF behavior. A complete circuit model of all distributed elements within the device (“white box model”) is highly complex and very difficult to achieve, but necessary for frequencies above roughly 100 MHz. Using the measurement data also allows to perform a black box modeling approach, which neglects all information about the internal structure. But this does not enable to adapt the simulation model to design changes quickly and easily, as they would lead to the necessity of re-measuring the black-box RF behavior. A compromise between these two opposing modeling approaches leads to a “grey box” model, which is much less complex and faster to achieve. This model has physical explanations in the dominant structures of the device, but abstracts fewer influential parts. The simulation model for the investigated inverter describes the internal structure with concentrated elements. This simplification is valid for structures smaller than $\lambda/6$, thus the model represents the inverter’s RF behavior up to ~200 MHz. The resulting electric equivalent circuit is shown in Figure 4.

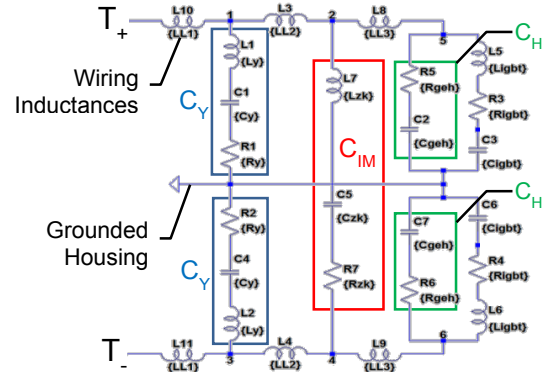


Figure 4. Electric equivalent circuit model of the investigated inverter, emulating the RF behavior in a frequency range of 300 kHz – 200 MHz

All wiring inside the model is represented with its parasitic inductances of around 10 nH/cm length. The applied capacitors C_Y and C_{IM} are modeled as series circuits of their nominal capacitance values, lead inductances and ohmic resistances.

The distributed capacitances between the conductors and the grounded housing are concentrated in one capacitor C_H , which is a simplification that limits the resulting model to frequencies lower than 200 MHz. The RF behavior of the semiconductor devices is modeled with a series circuit of their parasitic elements and their wiring. This simplification limits the validity of the simulation model to frequencies higher than approximately ten times the PWM frequency, here roughly around 100 kHz. Figure 5 shows a comparison of the CM impedances of the measurement versus a SPICE simulation.

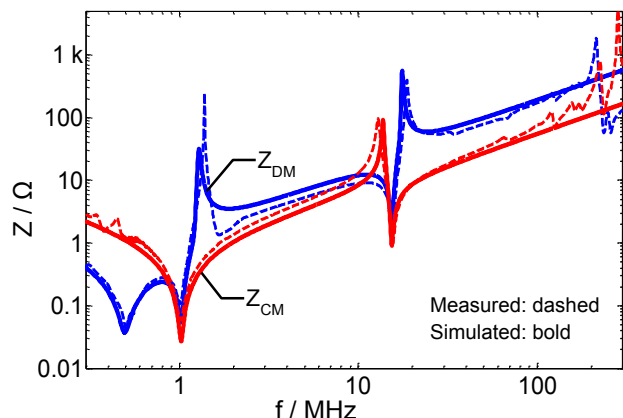


Figure 5. Comparison of the impedance curves between the inverter in the passive state and the simulation with the EMC model

Figure 5 shows a good similarity between the simulation model and measurement data over a broad frequency range. Smaller deviations at low frequencies are caused by measurement uncertainties (mainly calibration and limited measurement dynamics). As the simplified model does not represent the distributed elements sufficiently, additional resonances above 100 MHz cannot be modeled. However, as these resonances have much lower dominance, the model does not need to be extended for representing the impedance behavior above 100 MHz.

C. Summary of the Impedance Characterization of a Traction Inverter as a Passive Two-Port

The RF input impedance behavior of a HV inverter is characterized in the passive state with scattering parameter measurements. Its input impedance is mainly influenced by passive components, such as EMI capacitors and parasitic inductances of the internal wiring structures. The input capacitors C_Y are responsible for the main resonance around 1 MHz; the second main resonance around 15 MHz is formed by the capacitance between the grounded inverter housing (C_H) and the wiring of the B6-bridge. The semiconductor devices (IGBTs) are not the dominant part influencing the input impedance of the inverter. Therefore, it is assumed that the input impedance of the activated inverter, with switching semiconductors, is also dominated by its passive structures. Thus, the input impedance of the passive state might represent the series impedance of a Thévenin's equivalent circuit for the CM disturbance sources.

III. CALCULATION OF THE DISTURBANCE SOURCE IMPEDANCE IN AN ACTIVE STATE

The previous methodology of measuring scattering parameters and converting them into CM and DM impedances is not directly applicable for active devices. A clear separation of signals and disturbances is not possible, as the conducted emissions of the DUT interfere with the excitation of the VNA. Consequently a different measurement approach is needed.

A. Application of Thévenin's Law to describe Common Mode Disturbance Sources

Thévenin's law allows a simplification of complex electrical networks to an ideal voltage source plus one series impedance. Ideally, the source voltage U_0 can be determined by measuring the output voltage over an infinitesimal load. There is no voltage drop over the source impedance without current flowing and the output voltage is equal to the source voltage. Determining the short circuit current allows a calculation of the source impedance Z_L , because the source voltage is known and drives the short circuit current through the source impedance. Unfortunately, it is impossible to achieve these ideal load conditions for CM disturbance sources in a component level test setup. However, the methodology can be used for any load condition of the disturbance source using Kirchhoff's voltage law: The disturbance source and the load impedance form a circuit loop, therefore, two known load impedances Z_L are sufficient to determine the two unknown variables U_0 and Z_L [7]. These quantities are all complex and frequency dependent; therefore, it is also necessary to measure the load voltages as complex quantity over frequency. Additionally, the result is directly based on the load impedance Z_L , which means that a sufficiently accurate measurement is needed.

B. Component Level EMC Test Setup according to CISPR 25

The Thévenin's equivalent circuit of the DUT is intended to describe a CM disturbance source of a HV traction inverter. The measurement of conducted emissions requires a test setup which allows the traction system to be operated under a typical load condition. The setup shown in Figure 6 enables the inverter (DUT) to drive an electric machine (M) and complies with the specifications of CISPR 25 for component level EMC tests [8].

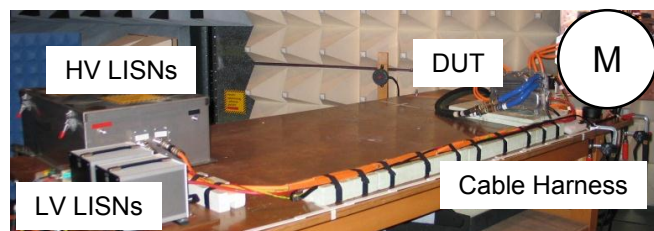


Figure 6. Photo of the measurement setup on a component level according to CISPR 25 for HV traction inverters

The DUT generates three-phase AC power to feed a synchronous traction machine (M). Two HV traction cables of 3.7 m length supply the inverter with DC. The HV and LV cables are bundled into one cable harness and the HV cables are terminated with line impedance stabilization networks (LISNs). The electric traction system drives a generator with a mechanical power of $P_m = 2.8$ kW outside the semi-anechoic

test chamber. The time domain voltages at the inverter's input ports T_+ and T_- are recorded using an oscilloscope for the calculation of the complex unknowns U_o and Z_I . The nodal voltages U_{T_+} and U_{T_-} are converted to modal voltages U_{CM} and U_{DM} as shown in [4], followed by a Fast Fourier Transformation into complex quantities of the frequency domain.

C. Measurement Results of the Active State

The input impedance of the attached HV cable equals the load impedance Z_L for the CM disturbance sources inside the DUT. The coaxial shielding of the HV cables leads to a transmission line behavior of the HV harness in the EMC frequency range [9]. The load impedance Z_L is dominated by the cable's termination, which can be varied, as shown in [5]. This method using a small filter PCB, allows the variation of the HV cables' termination. This termination is transformed into the cables' input impedance and, therefore, that method enables the adjustment of three different load conditions. As only two of them are required to solve the equation system, the resulting quantities U_o and Z_I are over-determined and a geometric mean value is calculated. Due to the limited measurement dynamics of the oscilloscope in the higher frequency range, the recorded CM disturbances are within the noise floor above 30 MHz. Multiple measurements were executed and the geometric mean value, respectively their standard deviation calculated to increase the dynamic range. The impedance Z_{G1} in the active state with its standard deviation is plotted in Figure 7.

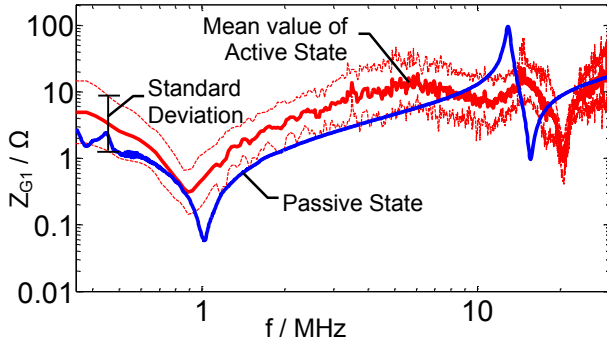


Figure 7. Calculated CM impedance Z_{G1} of the active inverter and the correspondent in its passive state. A frequency shift of ~ 100 kHz occurs

Figure 7 shows the mean value of the calculated source impedance as a thick red line. The thinner red lines are the mean value plus standard deviation (upper line), respectively minus standard deviation of 35 measurements in total. The blue line represents the CM input impedance of the inverter as a passive two-port. Both curves show a very similar impedance trend. The main resonance at 1 MHz is shifted by ~ 100 kHz, and the amplitude is slightly increased over the whole frequency range. This leads to the conclusion that the CM source impedance can be estimated with VNA measurements.

D. Summary of the Measurements in the Active State

The CM disturbance sources within an HV inverter can be modeled as a series connection of an ideal voltage source and one series impedance, which describes all non-ideal effects. It is possible to adjust different load impedances by varying the

termination impedance of the HV cables within a component level test setup. The values of the Thévenin's equivalent circuit can be calculated with time domain measurements. Compared to the CM input impedance of the same DUT in a passive state, the CM input impedance is very similar to the disturbance source's series impedance. Therefore, it is not necessary to carry out an elaborate CISPR 25 measurement to determine the source impedance. It is sufficient to value the CM input impedance using a VNA, avoiding the need for an inverter controlling bus system, DC supply and electric driving, respectively braking machines. The source voltage can be measured using an oscilloscope with a high ohmic (1 M Ω) voltage probe.

IV. PHYSICAL EMULATION OF THE INVERTER FOR FILTER DEVELOPMENT IN AUTOMOTIVE HV NETWORKS

The load impedance of a disturbance source determines the voltage emissions, respectively current amplitudes. Applying a filter to reduce conducted disturbances has two effects: Firstly, it changes the load condition for the disturbance source, because the new load impedance is a series connection of the filter circuit with the previous load impedance. Secondly, it changes the disturbance source of the inverter itself. As the filter is applied as a structure within the inverter's housing, the disturbance source emitting conducted EMI on HV cables is now a series connection of the filter circuit with the unchanged CM equivalent source. Thus, the knowledge of the impedances on both sides of the filter in its application environment is required for the optimization of the filter structures.

A. Physical Emulation of the Inverter's Source Impedance

Emulating a more realistic impedance environment for a HV filter allows the characterizing of a realistic attenuation curve. Therefore, most parts of the test setup can be used unchanged: The LISNs, shielded housings and HV cables are configured as stated by CISPR 25. The DC supplies, low voltage controlling bus and electric machines are no longer required and can be removed. As only conducted emissions are regarded, there is no need for a semi-anechoic chamber, but the conductive table is required. This represents an enormous simplification of the EMC test setup, but a realistic excitation is missing. The excitation device needs to generate a voltage and current spectrum, which is comparable to the inverter at a typical operation point. Its source impedance needs to equal the curves presented in previous chapters. Therefore, the SPICE simulation model of the inverter was built up using concentrated elements. This inverter emulating circuit is assembled as pictured in Figure 8, and its CM input impedance is plotted in Figure 9 (VNA measurement).

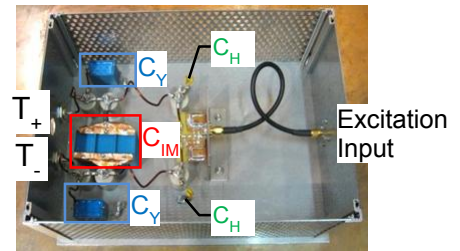


Figure 8. Physical buildup of the inverter simulation circuit

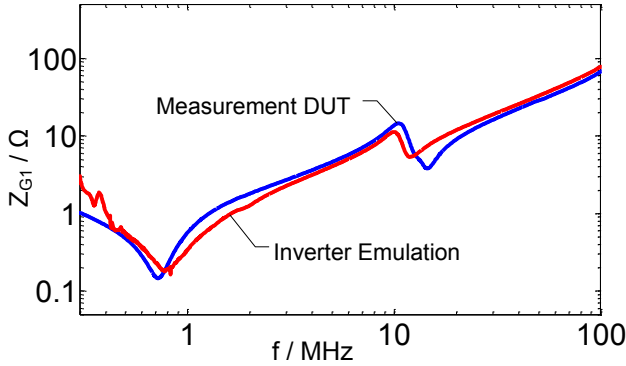


Figure 9. CM impedance Z_{G1} of the inverter emulation compared to the CM input impedance of the HV inverter

Figure 9 shows a close similarity of the input impedances of physical representation and DUT for most of the frequency range. As the leads of the emulation circuitry have a much lower diameter than the wiring within the HV inverter, the skin effect reduces the Q-factor of the resonances at 10–20 MHz. However, in summary, the inverter emulation features the same source impedance as the tested device.

B. Conducted Emissions of the Inverter Emulation

The physical representation of the simulation model emulates the inverter's input impedances. An appropriate excitation of this inverter emulation is required for the calculation of a filter's attenuation. An additional excitation port was included in the physical inverter model, as highlighted in Figure 8. A square pulse generator can be connected at this port. This excitation source needs to generate a similar time domain signal as the disturbances of the inverter within the operating point of the traction system. The test results of Figure 10 are recorded in a setup consisting of the pulse generator exciting the physical representation shown in Figure 8. This inverter emulation is connected to typical HV cables ($\ell = 3.7$ m) which are terminated with LISNs on a conductive table, according to CISPR 25 (recorded with an EMI test receiver, IFBW 120 kHz, peak detector).

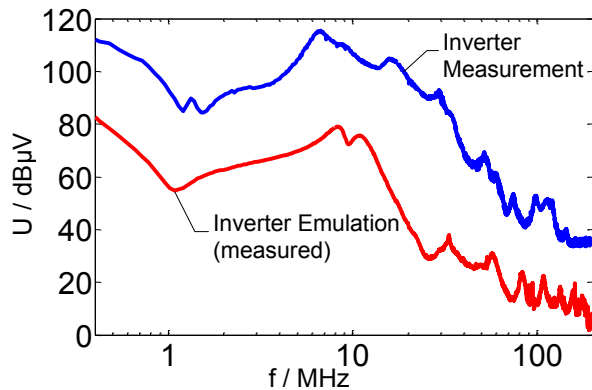


Figure 10. Conducted disturbance voltages of traction inverter and its EMC emulation; nearly constant difference of -35 dB occurs

The test results plotted in Figure 10 show the conducted emissions of the HV inverter in blue and its emulation in red. Obviously, the disturbance amplitudes of the real inverter are

higher than the emissions of the inverter emulation. This difference of ~ 35 dB is nearly constant over the entire frequency range. There is an increased difference only between 15–20 MHz, as the traction machine with its housing form a CM resonance within this range. This machine resonance is not represented by the inverter emulation. Additional measurements show that the amplitude difference of 35 dB is constant for varying load impedances and also appears in the current emissions. The difference of emitted disturbances arises by the limited output power of the impulse generator. Whereas the impulse generator delivers maximum voltages of 20 V, the power semiconductors induce a rectangular signal of 280 V, resulting in an excitation difference of 23 dB. The IGBTs are low resistive whilst conducting, thus they can be represented by a disturbance source with low series impedance. The impulse generator features a source impedance of 50 Ω , and these differences result in the total amplitude difference of 35 dB. A constant difference of disturbance amplitudes does not matter for linear filter devices: As long as the intended filter structure is linear (e.g. ferrite material not saturated), the filter attenuation is independent of the disturbance amplitudes.

C. Summary of the Physical Emulation of a Traction Inverter

A simplified SPICE model is developed with the measured input impedances of a traction inverter in the passive state. The simulation model is built up as a physical representation of the input impedances. An excitation of this circuit with rectangular pulses forms an inverter emulation. The disturbances emissions have a similar frequency spectrum at lower amplitudes and the emulation exhibits a similar RF source behavior regarding load changes and current emissions. This emulation enables to determine a filter's attenuation in a more realistic environment compared to the standard 50 Ω system, which is commonly used to measure the filter performance.

V. FILTER ATTENUATION MEASURED IN THE EMULATED ELECTRIC TRACTION SYSTEM ENVIRONMENT

The standard filter attenuation measurement method uses a VNA. This results in an attenuation curve, determined with a 50 Ω source impedance and a 50 Ω load attached to the filter circuit. However, measurements show that the HV cables input impedance differs significantly from 50 Ω in an EMC test setup [5]. This cable's input impedance loads the disturbance source within the EMC test. As shown previously, the CM source impedance also does not equal 50 Ω within the investigated frequency range. Hence the filter attenuation, measured in a 50 Ω system, may not be reproduced in a component level EMC test.

The only solution to determine the real filter attenuation is its application into the traction system and to measure the emissions spectra without filter and with filter applied. The subtraction of the test results yields an emission difference, which represents the real filter attenuation. To show this difference of filter performance, a commercial first-order low-pass EMI filter is investigated. This filter is inserted in between the inverter emulation and the HV cables. The conducted voltage emissions of the emulation are compared with and without this example filter applied. Figure 11 plots the test results appearing, measured with an EMI test receiver (IFBW 120 kHz, peak detector).

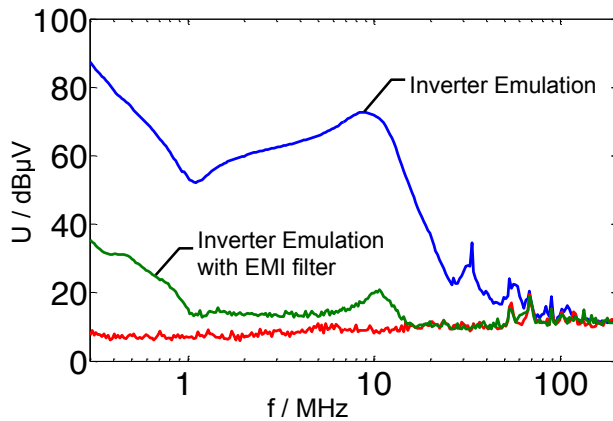


Figure 11. Frequency spectrum of the disturbance voltage at LISN unfiltered (blue curve) and with EMI filter implemented (noise level in red)

The unfiltered inverter emissions are plotted in blue, the filtered voltage disturbances are displayed in green and the noise level of the test setup is colored in red. The EMI filter reduces the voltage emissions by about 60 dB in the lower frequency range. The filtered emissions of the emulation above 15 MHz are below the noise level, and so there is no valid calculation of the filter's attenuation. Below this frequency, the disturbance difference of unfiltered and filtered emissions is equal to the filter attenuation, which is plotted as a red curve in Figure 12.

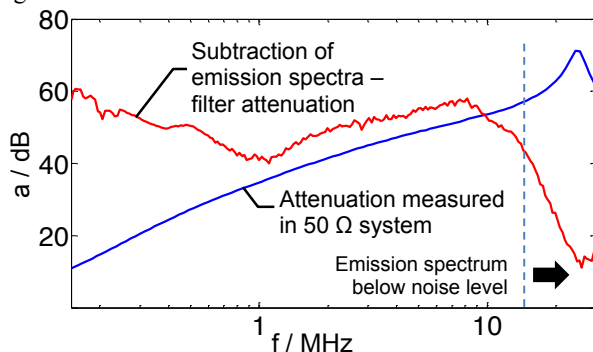


Figure 12. Filter attenuation measured with a VNA in the common 50 Ω system and emission spectrum difference when the filter is implemented in the inverter emulation

Figure 12 shows the attenuation of the filter used for this example in the inverter environment (red curve) compared to the attenuation in a 50 Ω system, displayed in blue. The first-order low-pass shows a nearly linear attenuation increasing up to ~20 MHz measured with a VNA. In contrast, the same filter shows significantly higher attenuation values and a decreasing filtering behavior up to the inverter's main resonance at 1 MHz. Above that, it shows a similar trend at slightly increased values. However, the filter attenuation decreases from a frequency of ~7 MHz, in contrast to the routine measurement. The spectrum difference above 15 MHz no longer represents the filter attenuation, as the filtered spectrum is below the noise level of the test setup. Thus, considering its trend and the behavior at lower frequencies, the filter attenuation is different when it is implemented in the inverter emulation.

VI. CONCLUSIONS AND OUTLOOK

The increasing electrification of the traction system in electric and hybrid driven vehicles results in more severe EMC problems. A reduction of EMI can be achieved with the application of line filters between the HV cables and the traction inverter, as its power semiconductors are the main EMI source within HV systems. The surrounding impedance situation has to be taken into account for effective filter development. According to Thévenin's theorem, the disturbance sources within a traction inverter can be modeled as an ideal voltage source with an equivalent series impedance.

In this contribution, the input impedances of a traction inverter is determined via network analyzer measurements and a following impedance calculation methodology. These measurements are executed in an unpowered state of the device. The source voltage and equivalent source impedance of the interference sources inside the inverter are quantified with time domain measurements of disturbances on HV traction lines. It is shown that the passive structures within the inverter dominate the source impedance.

An inverter emulation is built up of concentrated elements using a black box simulation model. This emulation has an equivalent EMC performance regarding conducted emissions on HV lines as the tested device. This model of the DUT is used to show the influence of surrounding impedances on the attenuation of a filter device. Deviations of more than 40 dB are shown. Therefore, the changed impedance situation can lead to compromised and ineffective EMC countermeasures.

VII. ACKNOWLEDGMENT

The authors would like to thank Robert Bosch GmbH for funding and supporting the EMC measurements of an automotive electric traction system.

VIII. REFERENCES

- [1] S. Guttowski, S. Weber, E. Hoene, W. John, and H. Reichl, "EMC issues in cars with electric drives," in *IEEE International Symposium on Electromagnetic Compatibility*, Boston, 2003, pp. 777 - 782, vol.2.
- [2] H. Rebholz and S. Tenbohlen, "Prospects and Limits of Common- and Differential-Mode Separation for the Filter Development Process," in *International Symposium on Electromagnetic Compatibility - EMC Europe*, Hamburg, 2008, pp. 1 - 6.
- [3] Mohamed F. Moad, "On Thevenin's and Norton's Equivalent Circuits," *Education, IEEE Transactions on*, vol. 25, no. 3, pp. 99 - 102, Aug. 1982.
- [4] C. Paul, *Introduction to Electromagnetic Compatibility*. New York: Wiley & Sons, 1983.
- [5] M. Reuter, S. Tenbohlen, and W. Köhler, "Influence of Termination Impedance on Conducted Emissions in Automotive High Voltage Networks," in *EMC Europe 2012*, Roma, 2012, p. 6.
- [6] P. Russer, *Electromagnetics, microwave circuit and antenna design for communications engineering*. Boston: Artech House, 2003.
- [7] C. Paul, *Fundamentals of electric circuit analysis*. New York: Wiley & Sons, 2001.
- [8] CISPR 25. (2008) Radio disturbance characteristics for the protection of receivers used on board vehicles, boats and on devices – Limits and methods of measurement. IEC/CISPR 25:2002 / DIN-EN 55025:2003.
- [9] M. Reuter, S. Tenbohlen, W. Köhler, and A. Ludwig, "Impedance Analysis of Automotive High Voltage Networks for EMC Measurements," in *EMC Europe 2011*, York, UK, 2011, p. 6.